



Published in final edited form as:

*Oncogene*. 2019 October ; 38(41): 6794–6800. doi:10.1038/s41388-019-0917-0.

## Spermidine/spermine N1-acetyltransferase 1 is a gene-specific transcriptional regulator that drives brain tumor aggressiveness

Vijay S. Thakur<sup>1</sup>, Brittany Aguila<sup>2</sup>, Adina Brett-Morris<sup>3</sup>, Chad J. Creighton<sup>4,5</sup>, Scott M. Welford<sup>1,6,\*</sup>

<sup>1</sup>Department of Radiation Oncology, Miller School of Medicine, University of Miami, Miami, FL 33136

<sup>2</sup>Department of Biochemistry, Case Western Reserve University, Cleveland, OH 44106

<sup>3</sup>Department of Pharmacology, Case Western Reserve University, Cleveland OH, 44106

<sup>4</sup>Dan L. Duncan Comprehensive Cancer Center, Baylor College of Medicine, Houston, TX 77030

<sup>5</sup>Department of Medicine, Baylor College of Medicine, Houston, TX 77030

<sup>6</sup>Sylvester Comprehensive Cancer Center, Miller School of Medicine, University of Miami, Miami, FL 33136

### Abstract

Spermidine/spermine N1-acetyltransferase 1 (SAT1), the rate limiting enzyme in polyamine catabolism, has broad regulatory roles due to near ubiquitous polyamine binding. We describe a novel function of SAT1 as a gene-specific transcriptional regulator through local polyamine acetylation. SAT1 expression is elevated in aggressive brain tumors and promotes resistance to radiotherapy. Expression profiling in glioma cells identified SAT1 target genes that distinguish high and low grade tumors, in support of the prognostic utility of SAT1 expression. We further discovered mechanisms of SAT1-driven tumor aggressiveness through promotion of expression of both DNA damage response pathways as well as cell cycle regulatory genes. Mechanistically, SAT1 associates specifically with the promoter of the MELK gene, which functionally controls other SAT1 targets, and leads biologically to maintenance of neurosphere stemness in conjunction with FOXM1 and EZH2. CRISPR knockin mutants demonstrate the essentiality of the polyamine acetyl transferase activity of SAT1 for its function as a transcriptional regulator. Together, the data demonstrate that gene-specific polyamine removal is a major transcriptional regulatory mechanism active in high grade gliomas that drives poor outcomes.

### Keywords

SAT1; SSAT; polyamines; MELK; brain tumors; glioma; transcription

---

Users may view, print, copy, and download text and data-mine the content in such documents, for the purposes of academic research, subject always to the full Conditions of use:[http://www.nature.com/authors/editorial\\_policies/license.html#terms](http://www.nature.com/authors/editorial_policies/license.html#terms)

\***Correspondence:** Dr. Scott M. Welford, Department of Radiation Oncology, Miller School of Medicine, University of Miami, Miami FL 33136; [scott.welford@med.miami.edu](mailto:scott.welford@med.miami.edu).

**Conflict of interest statement:** The authors declare no conflicts of interest.

## Introduction

Polyamines putrescine, spermidine, and spermine are small, positively-charged molecules present in millimolar amounts in cells that bind acidic macromolecules, and broadly regulate functions such as replication, translation, chromatin condensation. Polyamines are both essential for life, and facilitators of cell death, and are thus tightly regulated through synthesis, uptake, and degradation/secretion to maintain homeostatic levels<sup>15</sup>. SAT1 is the global polyamine rheostat, serving as the rate-limiting catabolic enzyme that acetylates spermine and spermidine, and primes them for either back-oxidation (spermine to spermidine, and spermidine to putrescine) or cellular efflux. SAT1 itself is highly regulated by polyamine concentrations, underscoring significant cellular investment in controlling polyamines<sup>14</sup>.

Polyamines and SAT1 are present in all cellular compartments<sup>8</sup>, but specific roles in different locations are not well-described. SAT1 has a role at the cell membrane, controlling motility by regulating a polyamine-sensitive potassium channel, and is recruited by interaction with  $\alpha 9\beta 1$  integrin<sup>6</sup>. SAT1 has also been found to interact with the membrane-bound diamine transporter SLC3A2<sup>19</sup>, and cytoplasmic HIF1 $\alpha$ <sup>1</sup> and eIF5A<sup>13</sup>; the latter of which is a target of SAT1 acetylation controlling translation. While SAT1 is found in the nucleus, and polyamine catabolism is critical for unwinding DNA<sup>8, 22</sup>, no localized nuclear functions have been thus far ascribed.

SAT1 has been implicated in cancer, affecting cell migration<sup>20</sup>, proliferation and response to ionizing radiation (IR)<sup>2</sup>. Our group found SAT1 through an shRNA screen to cause resistance to radiation in glioblastoma (GBM), and showed that SAT1 is critical for tumor growth. We found that SAT1 controls expression of BRCA1 through a transcriptional mechanism. The observation helped explain why SAT1-elevated tumors respond less well to radiotherapy/temozolomide than SAT1-reduced tumors. However, the finding also led to the question of how SAT1 controls gene expression, and what other genes are controlled by SAT1. In the present study, we performed expression profiling on SAT1 competent and deficient brain tumor cells and identified the breadth of SAT1-dependent genes. We confirmed regulation in multiple neurosphere lines, and evaluated expression of the genes in TCGA data of 677 brain tumors. Our studies delineate the mechanism of SAT1-mediated gene expression, uncovering an unknown function of SAT1 in general, but also exposing SAT1 as a veritable therapeutic target in GBM that controls tumor cell stemness and aggressiveness.

## Results

### SAT1 regulates gene programs controlling cell cycle and DNA dynamics

In order to assess the extent of genes regulated by SAT1 in brain tumors, we performed gene expression profiling of U87MG cells with two shRNAs to SAT1 using Affymetrix microarrays covering 67,528 gene transcripts. U87MG cells were stably transduced with lentiviruses expressing shRNAs to either the green fluorescent protein (GFP) or SAT1, and RNA was harvest within 7 days of infection. RNA was reverse transcribed into cDNA, labelled with biotin and hybridized onto the arrays for analyses. Hierarchical clustering of

duplicate experiments correctly segregated samples according to sample identity (i.e. shGFP clustered together, shSAT1-1 clustered together, and shSAT1-2 clustered together; with the latter two separately branching from shGFP) (Figure 1A). At a fold-difference of  $\geq 2.5$ , and an ANOVA  $p$  value of  $\leq 0.07$ , 169 genes were differentially expressed between control and the shRNA cell lines (Supplementary Table 1), including previously identified BRCA1. At a threshold of 2.0, 332 genes were identified.

To validate gene expression changes in U87MG cells, we tested SAT1 knock down on a cohort of genes in two neurosphere lines (GBM821 and GBM913) that retain characteristics of tumor stem cells *in vivo*<sup>7</sup>. All of the genes demonstrated significant reductions in expression upon knock down of SAT1 (Figure 1B). We also validated that reduction of transcript resulted in decreased protein for several of the genes by Western blot (Figure 1C). Finally, to gain insight into the functions of the genes affected by SAT1, we performed gene ontology-based functional classification and found significant over-representation of genes involved in both cell cycle/mitosis/cytokinesis and DNA metabolism/replication/repair over all other categories (Figure 1D). Since we found previously that SAT1 regulates DNA repair and tumor growth, the data support a broad effect of SAT1 on genes driving aggressive tumor biology.

### **SAT1 target genes are enriched in high grade gliomas**

To glean clinical relevance for SAT1 target genes we queried TCGA and assessed expression in 677 gliomas. SAT1 is significantly overexpressed in high-grade glioblastoma compared to all subtypes of low-grade gliomas (Figure 2A). Furthermore, SAT1 expression correlates with poor outcome in the LGG + GBM (Low-Grade Glioma and Glioblastoma) cohort with a high level of significance ( $p < 0.001$ , log rank test) (Figure 2B), largely because when ranked by SAT1 expression levels, 80% of the glioblastomas segregate to the upper-third of the tumors, and only 4.9% fall to the lower-third. Considering only the low-grade gliomas, high SAT1 tumors again perform significantly worse than those with lower SAT1 levels ( $p = 0.001$ , log rank test) (Figure 2C). Notably, SAT1 expression was only prognostic in IDH1 wild type tumors, which tend to have poorer outcomes than IDH1 mutant (Figure 2D–E). Thus, SAT1 expression predicts poor outcome in human gliomas.

We next assessed the expression of the 152 SAT1 target genes (2.5-fold genes) that mapped to the TCGA dataset in each of the tumors in the LGG+GBM cohort that were clustered according a recent integrative analysis producing four grade-independent subtypes (LGr1–4)<sup>3</sup>. We noted strikingly that expression of the SAT1 genes was independent of subtype and distinctly higher in the GBM subset compared to the LGG subsets. Further among LGG, some of the LGr4 samples appeared more similar to the GBM samples, which are themselves comprised mostly of LGr4 (Figure 2D). Together the data demonstrate that SAT1 and its target genes are expressed in more aggressive gliomas (i.e. GBM) and portend poor prognosis in the LGG groups.

### **SAT1 regulates MELK and EZH2 by direct interaction with chromatin**

Intriguingly, MELK, FOXM1, EZH2, NEK2, and PLK1 are SAT1 target genes. Recent studies have demonstrated a role for the maternal embryonic leucine zipper kinase (MELK)

in brain tumors. MELK was shown to phosphorylate the FOXM1 transcription factor, leading to expression of EZH2, the catalytic subunit of the polycomb repressive complex PRC2<sup>11</sup>. All three proteins are necessary for stem cell maintenance, tumor growth, and resistance to IR. FOXM1 regulates proliferation by controlling polo-like kinase 1 (PLK1) during mitosis<sup>10</sup>, and NIMA-related kinase 2 (NEK2) is a regulatory binding partner of EZH2 in glioma stem cells<sup>21</sup>. Together, the MELK network promotes tumor aggressiveness.

We explored the interaction of MELK, FOXM1 and EZH2 at the gene expression level in three established cell lines (U87MG, LN229, and Gli36), and observed that knockdown of MELK caused reductions in expression of FOXM1, EZH2, and BRCA1 (Figure 3A). We next targeted FOXM1 by shRNA and found similarly that MELK, EZH2 and BRCA1 were again reduced as a consequence (Figure 3B). These data support published findings of a functional dependence/interaction between MELK and FOXM1<sup>10</sup>, and also that MELK and FOXM1 control each other at the transcriptional level<sup>11</sup>. We next investigated how SAT1 regulates expression of MELK and FOXM1, and performed chromatin immunoprecipitation (ChIP) to ask if SAT1 interacts with the proximal promoter regions of several of its targets. Using shGFP U87MG and shSAT1 U87MG, we found an association of SAT1 with both the MELK and EZH2 promoters, but not FOXM1, BRCA1, or NUSAP1 (Figure 3C). This observation led to the hypothesis that MELK and EZH2 are major nodes of SAT1 gene regulation, and the data in Figure 3A would suggest MELK precedes EZH2. We then tested the effect of MELK knockdown in comparison to SAT1 knockdown over a range of identified target genes across the three cell lines. We found in all genes tested, MELK knockdown with two shRNAs phenocopied SAT1 knockdown (Figure 3D). Interestingly, ectopic expression of MELK induced SAT1 target genes, but in an SAT1-dependent manner (Supplementary figure 1); suggesting MELK is necessary but not sufficient to drive SAT1 genes. To gain a broader view of the roles of MELK/FOXM1 and EZH2 in SAT1 driven gene expression programs, we analyzed recently published ChIPseq data for both FOXM1<sup>4</sup> and H3K27me3<sup>17</sup> (the EZH2-directed histone modification) in cancer cells, and compared their target genes to SAT1 target genes. Roughly one fifth (59 of 315, or 18.7%) of the SAT1 genes ( $\geq 2$  change) were identified to have FOXM1 binding (Figure 3E, and Supplementary Table 2); and one twentieth (17 of 315, or 5.4%) of the published EZH2 targets were found on the SAT1 gene list. To verify the effect of SAT1 knockdown on FOXM1 occupancy, we performed FOXM1 ChIP on three of its identified targets (CCNB1, CCNB2, and CDC20) and found reduced association of FOXM1 (Figure 3F). Finally, because MELK, FOXM1 and EZH2 have been associated with stemness of glioblastoma cells, we assessed the ability of SAT1 knockdown primary glioblastoma lines to form neurospheres in culture. In both the GBM821 and GBM913 lines, we found that SAT1 depletion led to significant reductions in the ability to form neurospheres (Figure 3G–H). Therefore, the data demonstrate that MELK and EZH2 are key drivers of SAT1-mediated gene regulation and biology, promoting brain tumor stemness.

### **SAT1 regulates transcription of specific targets through polyamine catabolism**

SAT1 is a polyamine catabolic enzyme. To assess the role of polyamines in SAT1-directed gene expression, we treated U87MG cells with 100  $\mu$ M spermidine (SPD) for 2, 4, or 6 hours, and harvested RNA for analysis. Notably, SAT1 itself is highly responsive to excess

polyamines<sup>14</sup>, and we observed rapid induction of SAT1 mRNA (Figure 4A). Similarly, we saw an induction of SAT1 targets BRCA1, MELK and EZH2. To determine if SAT1 was required for induction of the genes, or whether polyamines were responsible independently to induce transcription, we tested SAT1 knockdown cells and found a loss of responsiveness for all genes. The data argue that polyamine stimulation of SAT1 is required, but do not delineate whether catabolism of polyamines is involved. To determine if SAT1 polyamine acetylation activity is required for target gene activation, we created a conditional CRISPR/Cas9 knockin cell line in which wild type SAT1 remains expressed by its endogenous promoter until CRE recombinase induces excision of wild type exons 4–6, resulting in inclusion of mutant exons 4–6 with point mutations in both the acetyl Co-A and polyamine binding sites (R101A and E152K, respectively) (Figure 4C). The mutations have been shown to abrogate polyamine catabolism of SAT1<sup>5</sup>. To validate the cell line, adenoviral mediated expression of CRE recombinase was used, and genomic PCR was performed using primer sets A-B and A-C, as indicated in Figure 4C. The A-B primer pair only amplifies the target prior to recombination, while A-C amplifies after recombination. As seen in Figure 4D, virtually complete recombination was evidenced by the lack of signal in the A-B PCR post-recombination. We also validated that the resulting locus contained the designed mutations by Sanger sequencing the PCR products (Figure 4E). We then assessed the transcriptional activity of SAT1 mutants. As seen in Figure 4F–G, CRE recombination resulted in a moderate increase in SAT1 expression compared to control cells, but a dramatic loss of expression of both MELK and FOXM1 at both the mRNA and protein levels. The increase of SAT1 expression conforms with the production of non-functional SAT1, to which the cells respond by attempting to elevate expression. The loss of MELK and FOXM1 expression demonstrates that polyamine catabolism is required for transcriptional activation.

## Discussion

We have uncovered a novel function for SAT1 as a gene-specific transcriptional modulator. Depletion of SAT1 from cells revealed altered gene expression programs that include cell cycle regulation and DNA repair, which portend poor prognosis in brain tumors. Physical association of SAT1 with the MELK and EZH2 promoters, and the requirement of SAT1 enzymatic function to regulate genes support a model in which localization of SAT1 to target genes, and acetylation and removal of polyamines from chromatin promote transcriptional activation. The studies highlight an expanding role for polyamine metabolism in cancer, and support pathway modulators as potential therapeutics.

How SAT1 is recruited to specific sites on DNA, and whether SAT1 transcriptional programs in different tissues are unique are open questions; analysis of SAT1 binding partners in different contexts will likely lend insight. The only reported mechanism of functional localization of SAT1 is for cell motility, wherein SAT1 has been shown to interact with  $\alpha 9\beta 1$  integrin. As SAT1 does not have an identifiable DNA binding domain, protein-protein interaction is the likely mechanism to interact with chromatin. Additionally recent studies have highlighted differential affinities of DNA sequences for polyamines, such that AT-rich regions bind more strongly than GC-rich regions; and polyamine binding stabilizes DNA duplexes<sup>22</sup>. The significance of this is that SAT1-mediated acetylation and removal of polyamines could be sequence-dependent, offering a potential mode of specificity for

transcriptional activity, and a differential role of SAT1 on different genes. Interestingly, while we found MELK inhibition to phenocopy SAT1, and that ectopic expression of MELK elevated SAT1 target genes, MELK was insufficient to restore function in absence of SAT1. This suggests SAT1 function is still required beyond the control of MELK. Understanding exactly where SAT1 is needed in chromatin could illuminate a novel mechanism of epigenetic-like regulation of chromatin compaction and relaxation.

For brain tumors, the data presented argue that SAT1 function controls two major pathways, both of which are implicated in tumor aggressiveness and therapeutic resistance. Roughly 25% of SAT1 genes are direct targets of FOXM1 or EZH2. Some of the targets are transcription factors themselves, including DEPDC1<sup>9</sup> and TSHZ2<sup>16</sup>; thus it is conceivable that FOXM1/EZH2 account for virtually all of the SAT1 targets. With the negative association of SAT1 expression and patient outcome, focusing therapeutic strategies on MELK, FOXM1, and EZH2, for which inhibitors currently exist, may be therapeutically advantageous. Whether inhibition of SAT1 rather than these three targets would be more efficacious will require further study, but expanding the list of viable therapeutic targets is an advance in a disease in need of novel approaches.

## Materials and Methods

### Cells and Neurospheres

U87MG and LN229 (ATCC), and Gli36 (gift of Dr. Susanne Brady-Kalnay) cells were maintained in DMEM 10%FCS. GBM821 and GBM913<sup>7</sup> neurospheres were grown in neuro stem cell media<sup>7</sup>. shRNAs were acquired from Sigma (supplementary material). For neurosphere quantification, the media contained 1.5% methyl-cellulose; spheres were scored after 12 days with Metamorph software. pCSII-IB-MELK was a gift of Dr. Takeuchi<sup>18</sup>.

### Microarray analyses

RNA was processed and hybridized at the CWRU Integrated Genomics Shared Resource. Analyses were performed using Transcriptome Analysis Console (Affymetrix), the PANTHER Classification System ([www.pantherdb.org](http://www.pantherdb.org)), and the Xena Functional Genomics Explorer ([xenabrowser.net](http://xenabrowser.net)).

### Statistics

Statistical tests were performed with Graphpad Prism 7.0 as indicated for each figure. All assays were repeated with both technical and biological replicates (n ≥ 3).

### ChIP/RT-PCR/Western Blotting

ChIP was described previously<sup>12</sup>. For antibodies and RT-PCR primers, see supplementary material.

### CRISPR

Knockin vectors were constructed in pBSKSII+ with a BSR cassette flanking mutated exons 4–6. The gRNA sequence targeting the PAM sequence GGAATACGTCAGGTTTACACGG within intron 3 of *SAT1* was used to design an



sgRNA by *in vitro* transcription, and was transfected with CAS9 and linearized vector into U87MG cells. Individual blasticidin-resistant clones were screened by PCR. Recombination was induced with Ad5CMVCre-eGFP (University of Iowa).

## Supplementary Material

Refer to Web version on PubMed Central for supplementary material.

## Acknowledgments

This work was supported by P30CA125123 (CJC); and R01CA187053 (SMW).

## References

1. Baek JH, Liu YV, McDonald KR, Wesley JB, Zhang H, Semenza GL. Spermidine/spermine N(1)-acetyltransferase-1 binds to hypoxia-inducible factor-1alpha (HIF-1alpha) and RACK1 and promotes ubiquitination and degradation of HIF-1alpha. *The Journal of biological chemistry* 2007; 282: 33358–33366. [PubMed: 17875644]
2. Brett-Morris A, Wright BM, Seo Y, Pasupuleti V, Zhang J, Lu J et al. The polyamine catabolic enzyme SAT1 modulates tumorigenesis and radiation response in GBM. *Cancer research* 2014; 74: 6925–6934. [PubMed: 25277523]
3. Ceccarelli M, Barthel FP, Malta TM, Sabedot TS, Salama SR, Murray BA et al. Molecular Profiling Reveals Biologically Discrete Subsets and Pathways of Progression in Diffuse Glioma. *Cell* 2016; 164: 550–563. [PubMed: 26824661]
4. Chen X, Muller GA, Quaas M, Fischer M, Han N, Stutchbury B et al. The forkhead transcription factor FOXM1 controls cell cycle-dependent gene expression through an atypical chromatin binding mechanism. *Molecular and cellular biology* 2013; 33: 227–236. [PubMed: 23109430]
5. Coleman CS, Huang H, Pegg AE. Structure and critical residues at the active site of spermidine/spermine-N1-acetyltransferase. *The Biochemical journal* 1996; 316 ( Pt 3): 697–701. [PubMed: 8670140]
6. deHart GW, Jin T, McCloskey DE, Pegg AE, Sheppard D. The alpha9beta1 integrin enhances cell migration by polyamine-mediated modulation of an inward-rectifier potassium channel. *Proc Natl Acad Sci U S A* 2008; 105: 7188–7193. [PubMed: 18480266]
7. Galli R, Binda E, Orfanelli U, Cipelletti B, Gritti A, De Vitis S et al. Isolation and characterization of tumorigenic, stem-like neural precursors from human glioblastoma. *Cancer research* 2004; 64: 7011–7021. [PubMed: 15466194]
8. Holst CM, Nevsten P, Johansson F, Carlemalm E, Oredsson SM. Subcellular distribution of spermidine/spermine N1-acetyltransferase. *Cell biology international* 2008; 32: 39–47. [PubMed: 17920945]
9. Huang L, Chen K, Cai ZP, Chen FC, Shen HY, Zhao WH et al. DEPDC1 promotes cell proliferation and tumor growth via activation of E2F signaling in prostate cancer. *Biochemical and biophysical research communications* 2017; 490: 707–712. [PubMed: 28634077]
10. Joshi K, Banasavadi-Siddegowda Y, Mo X, Kim SH, Mao P, Kig C et al. MELK-dependent FOXM1 phosphorylation is essential for proliferation of glioma stem cells. *Stem cells* 2013; 31: 1051–1063. [PubMed: 23404835]
11. Kim SH, Joshi K, Ezhilarasan R, Myers TR, Siu J, Gu C et al. EZH2 protects glioma stem cells from radiation-induced cell death in a MELK/FOXM1-dependent manner. *Stem cell reports* 2015; 4: 226–238. [PubMed: 25601206]
12. Krieg AJ, Hammond EM, Giaccia AJ. Functional analysis of p53 binding under differential stresses. *Molecular and cellular biology* 2006; 26: 7030–7045. [PubMed: 16980608]
13. Lee SB, Park JH, Folk JE, Deck JA, Pegg AE, Sokabe M et al. Inactivation of eukaryotic initiation factor 5A (eIF5A) by specific acetylation of its hypusine residue by spermidine/spermine acetyltransferase 1 (SSAT1). *The Biochemical journal* 2011; 433: 205–213. [PubMed: 20942800]

14. Pegg AE. Spermidine/spermine-N(1)-acetyltransferase: a key metabolic regulator. *American journal of physiology Endocrinology and metabolism* 2008; 294: E995–1010. [PubMed: 18349109]
15. Pegg AE, Casero RA Jr. Current status of the polyamine research field. *Methods in molecular biology* 2011; 720: 3–35. [PubMed: 21318864]
16. Santos JS, Fonseca NA, Vieira CP, Vieira J, Casares F. Phylogeny of the teashirt-related zinc finger (tshz) gene family and analysis of the developmental expression of tshz2 and tshz3b in the zebrafish. *Dev Dyn* 2010; 239: 1010–1018. [PubMed: 20108322]
17. Sharma V, Malgulwar PB, Purkait S, Patil V, Pathak P, Agrawal R et al. Genome-wide CHIP-seq analysis of EZH2-mediated H3K27me3 target gene profile highlights differences between low- and high-grade astrocytic tumors. *Carcinogenesis* 2017; 38: 152–161. [PubMed: 27993893]
18. Takeuchi H, Saito H, Noda T, Miyamoto T, Yoshinaga T, Terahara K et al. Phosphorylation of the HIV-1 capsid by MELK triggers uncoating to promote viral cDNA synthesis. *PLoS pathogens* 2017; 13: e1006441. [PubMed: 28683086]
19. Uemura T, Yerushalmi HF, Tsaprailis G, Stringer DE, Pastorian KE, Hawel L 3rd et al. Identification and characterization of a diamine exporter in colon epithelial cells. *The Journal of biological chemistry* 2008; 283: 26428–26435. [PubMed: 18660501]
20. Veeravalli KK, Ponnala S, Chetty C, Tsung AJ, Gujrati M, Rao JS. Integrin alpha9beta1-mediated cell migration in glioblastoma via SSAT and Kir4.2 potassium channel pathway. *Cellular signalling* 2012; 24: 272–281. [PubMed: 21946432]
21. Wang J, Cheng P, Pavlyukov MS, Yu H, Zhang Z, Kim SH et al. Targeting NEK2 attenuates glioblastoma growth and radioresistance by destabilizing histone methyltransferase EZH2. *The Journal of clinical investigation* 2017; 127: 3075–3089. [PubMed: 28737508]
22. Yoo J, Kim H, Aksimentiev A, Ha T. Direct evidence for sequence-dependent attraction between double-stranded DNA controlled by methylation. *Nat Commun* 2016; 7: 11045. [PubMed: 27001929]



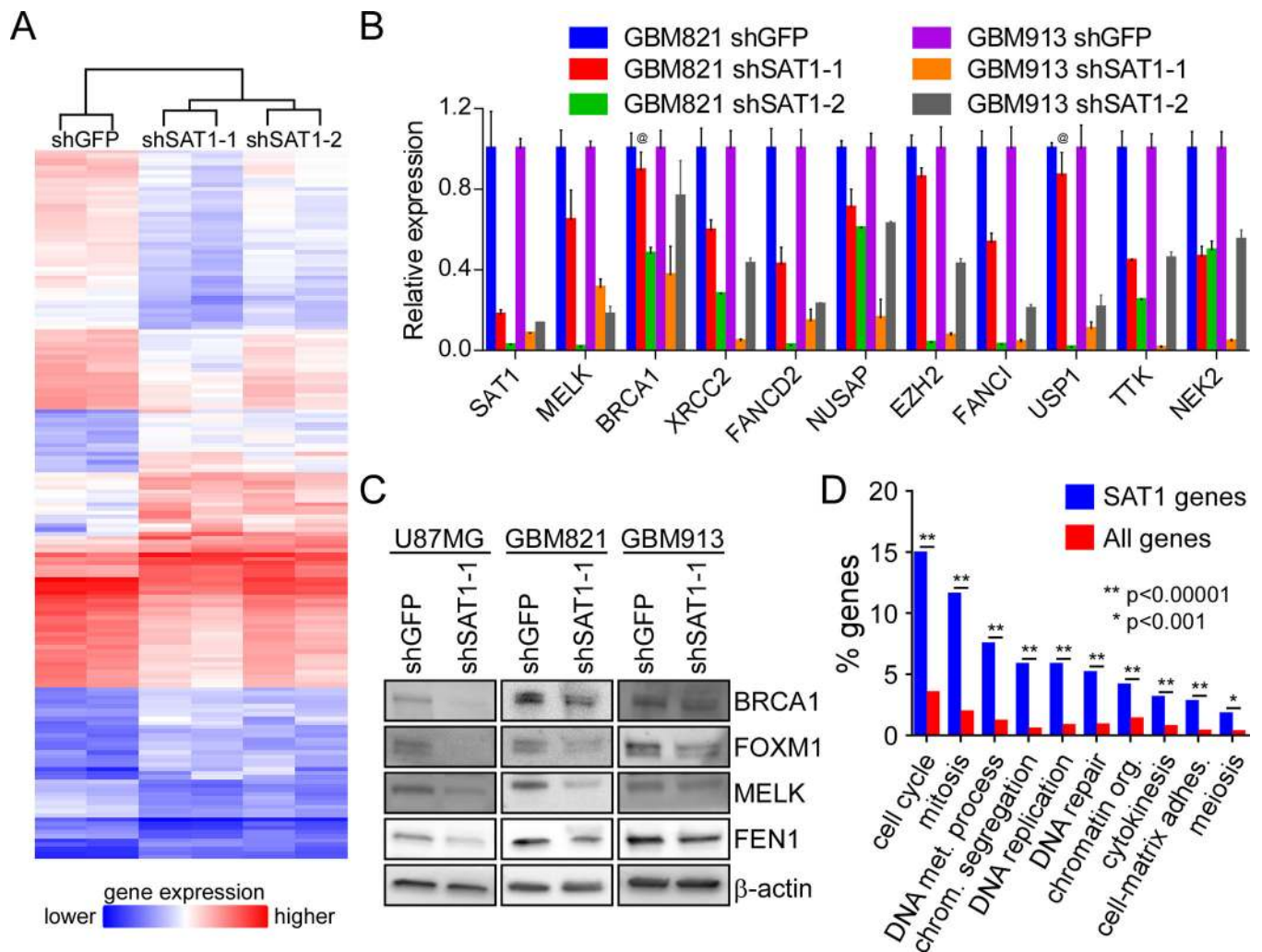


**Figure 1: SAT1 regulates cell cycle and DNA regulatory genes in GBM cells:**

A) Hierarchical clustering of differentially expressed genes from microarray data from U87MG cells expression shGFP or one of two shSAT1 shRNAs. Gene names are included in supplementary table 1. B) Validation of SAT1 target genes in two neurosphere lines by qRT-PCR.  $p < 0.05$  for all genes in the knockdown experiments except for those indicated by “@.” C) Validation of SAT1 target genes by Western blot. D) Gene ontology classification of SAT1 target genes (blue) into functional groups compared to all genes in the genome (red). Statistically significant differences are indicated.

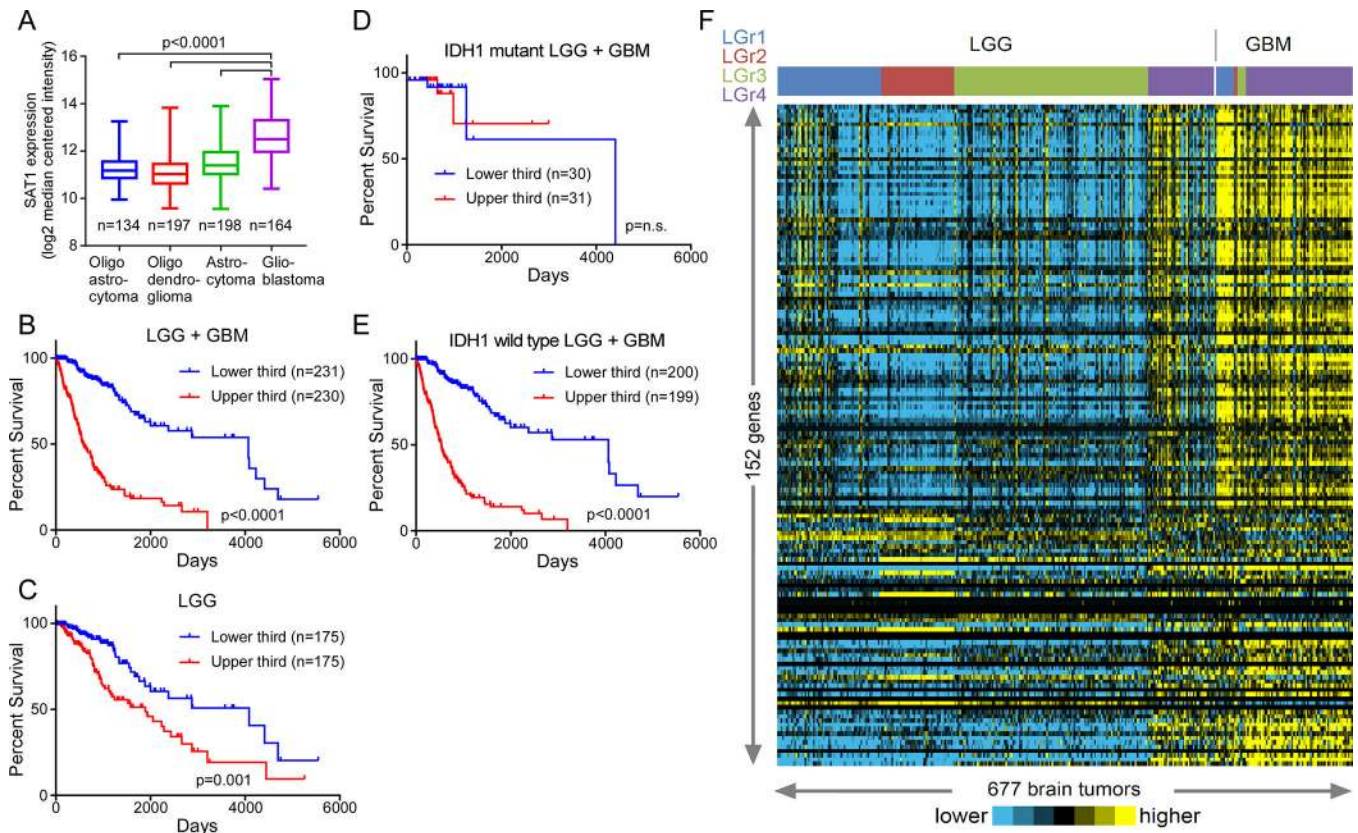


**Figure 2: SAT1 target genes are elevated in aggressive brain tumors:**

A) The expression of SAT1 in low and high grade gliomas from the TCGA LGG+GBM database. Pairwise statistical comparisons of low grade glioma to GBM are indicated (student's t-tests). B) Kaplan-Meier survival plot for low and high grade gliomas dichotomized by SAT1 expression. C) Kaplan-Meier survival plot for only low grade gliomas dichotomized by SAT1 expression. D) Kaplan-Meier survival plot for low and high grade IDH1 mutant gliomas dichotomized by SAT1 expression. E) Kaplan-Meier survival plot for low and high grade IDH1 wild type gliomas dichotomized by SAT1 expression. F) Expression of SAT1 target genes in 677 brain tumors of both low and high grades, organized by LGr classifications.

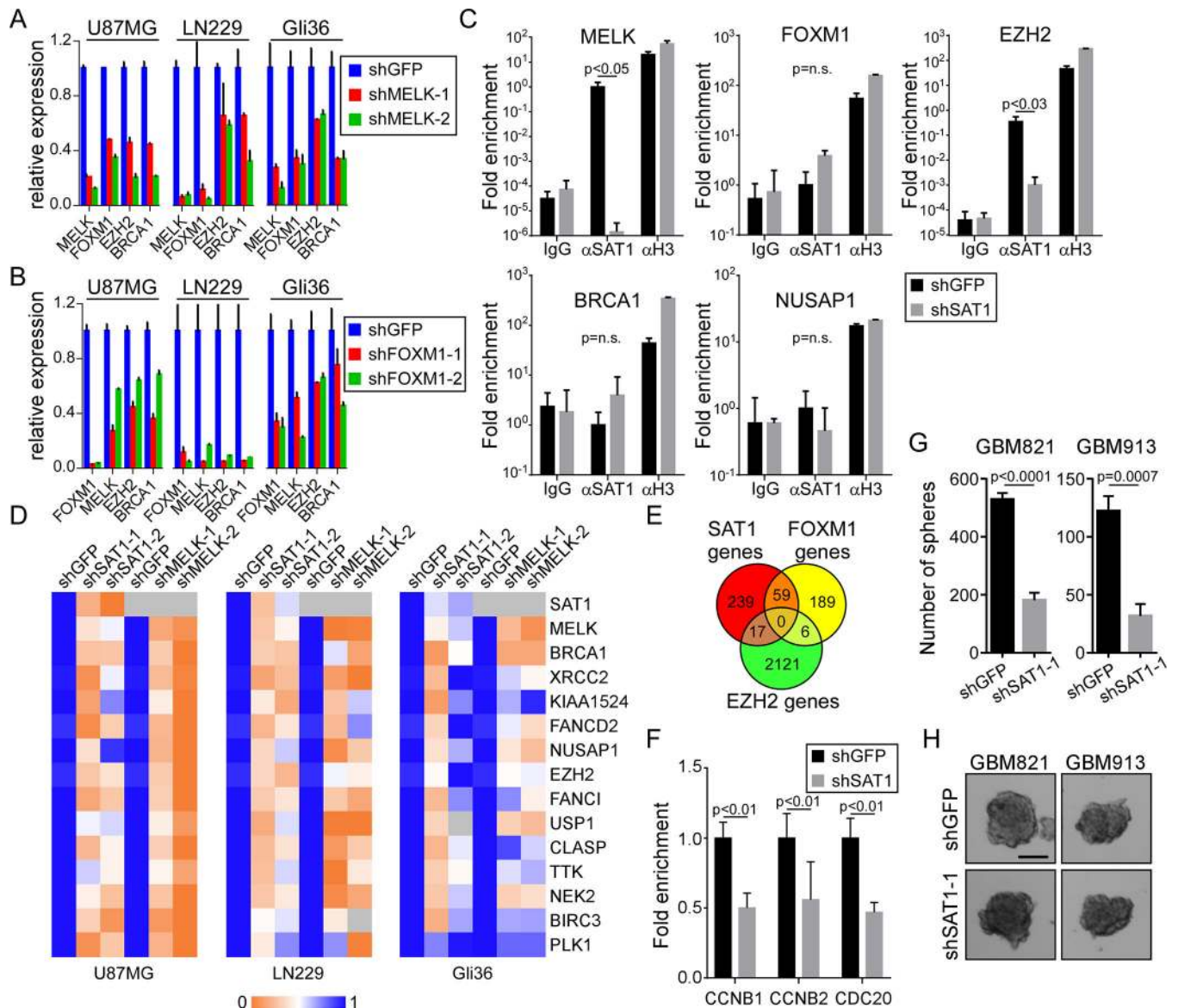


**Figure 3: MELK and EZH2 are SAT1 direct target nodes:**

A) Assessment of FOXM1, EZH2, and BRCA1 in control (shGFP) and MELK knockdown U87MG, LN229 and Gli36 cells by qRT-PCR.  $p < 0.05$  for all genes in the knockdown experiments. B) Assessment of MELK, EZH2, and BRCA1 in shGFP and shFOXM1 U87MG, LN229 and Gli36 cells by qRT-PCR.  $p < 0.05$  for all genes in the knockdown experiments. C) Input normalized SAT1 ChIP assay on U87MG shGFP and shSAT1 cells on the MELK, FOXM1, EZH2, BRCA1, and NUSAP1 promoters. Histone H3 ChIP is a positive control. D) Heat map of expression of SAT1 targets measured by RTPCR in shSAT1 U87MG, LN229 and Gli36 cells compared to shMELK cells. E) Venn diagram comparing SAT1 target genes with published FOXM1 and EZH2 targets. F) FOXM1 ChIP in shGFP and shSAT1 U87MG cells. G) Neurosphere formation assay in GBM821 and GBM913 lines with shGFP or shSAT1-1. H) Photomicrographs of neurospheres. Scale bar 100  $\mu$ m



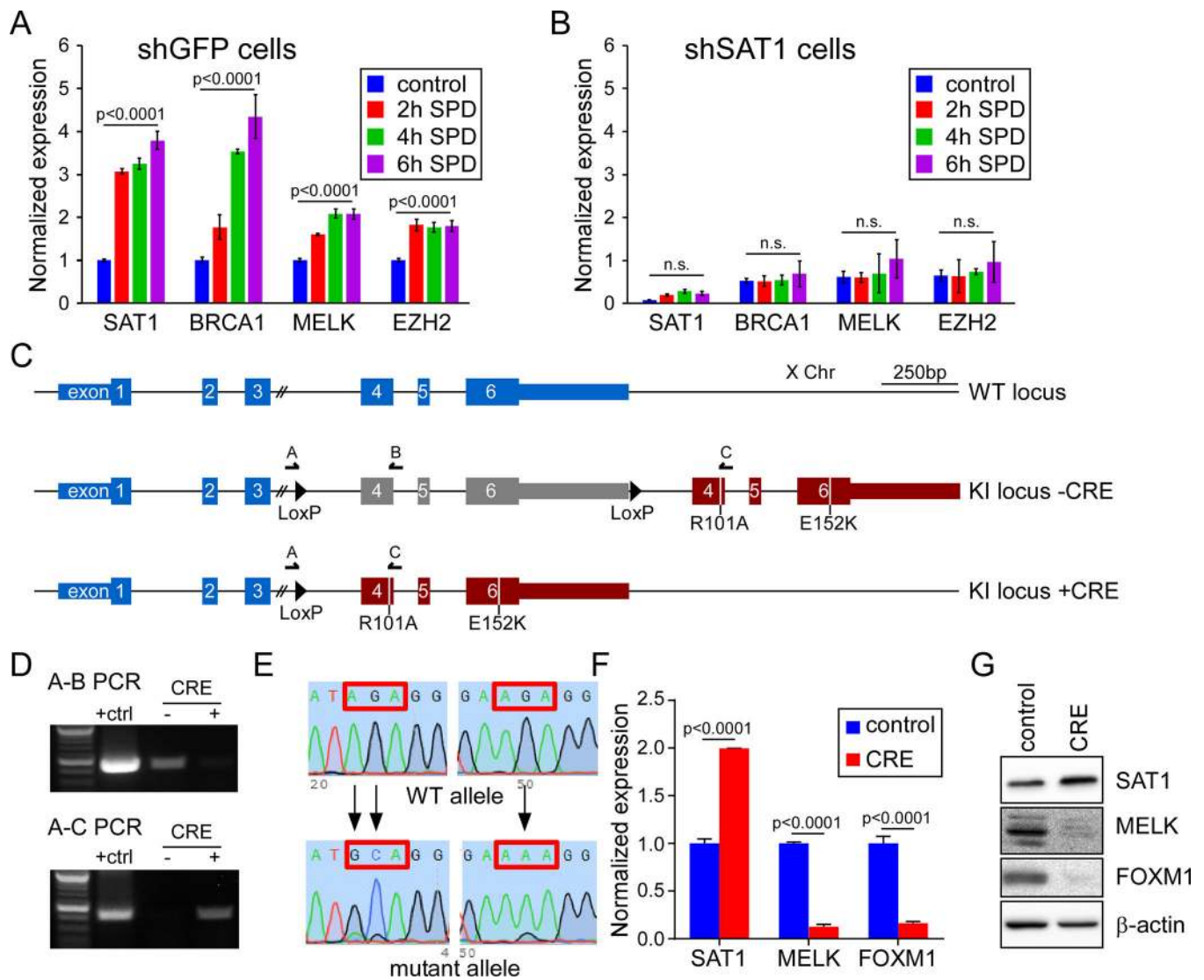


**Figure 4: Polyamine catabolism is necessary for SAT1 transcriptional activity.**

A, B) Measurement of SAT1 target genes after exposure to spermidine (SPD) by qRT-PCR in shGFP cells (A) or shSAT1 cells (B). C) Schematic of the SAT1 locus on the X Chromosome (top) and the modified locus after CRISPR/Cas9 induced knockin pre (middle) and post (lower) CRE recombination. D) PCR validation of recombination using primers indicated in the schematic. E) Sanger sequencing of the wild type and two mutations sites in the SAT1 after CRE recombination. F, G) Measurement of SAT1, MELK, and FOXM1 by qRT-PCR (F) and Western blot (G) in control or CRE adenovirus infected cells.